REPORT DOCUMENTATION PAGE

Form Approved
OMB No. 0704-0188

1. AGENCY USE ONLY *(LEAVE BLANK)*	2. REPORT DATE	3. REPORT TYPE AND DATES COVERED
	1998	Professional Paper

4. TITLE AND SUBTITLE
Nonlinear Adaptive Flight Control With A Backstepping Design Approach

5. FUNDING NUMBERS

6. AUTHOR(S)
Marc L. Steinberg and Anthony B. Page

7. PERFORMING ORGANIZATION NAME(S) AND ADDRESS(ES)
Naval Air Warfare Center Aircraft Division
22347 Cedar Point Road, Unit #6
Patuxent River, Maryland 20670-1161

8. PERFORMING ORGANIZATION REPORT NUMBER

9. SPONSORING/MONITORING AGENCY NAME(S) AND ADDRESS(ES)

10. SPONSORING/MONITORING AGENCY REPORT NUMBER

11. SUPPLEMENTARY NOTES

12a. DISTRIBUTION/AVAILABILITY STATEMENT
Approved for public release; distribution is unlimited.

12b. DISTRIBUTION CODE

13. ABSTRACT *(Maximum 200 words)*

14. SUBJECT TERMS

15. NUMBER OF PAGES

16. PRICE CODE

17. SECURITY CLASSIFICATION OF REPORT	18. SECURITY CLASSIFICATION OF THIS PAGE	19. SECURITY CLASSIFICATION OF ABSTRACT	20. LIMITATION OF ABSTRACT
Unclassified	Unclassified	Unclassified	SAR

NONLINEAR ADAPTIVE FLIGHT CONTROL WITH A BACKSTEPPING DESIGN APPROACH

Marc L. Steinberg[1] and Anthony B. Page[2]
Bldg 2187, CST 5, Naval Air Systems Command, Patuxent River, MD 20670

Abstract

This paper examines the use of adaptive backstepping for multi-axis control of a high performance aircraft. The control law is demonstrated on a 6 Degree-of-Freedom simulation with nonlinear aerodynamic and engine models, actuator models with saturation, and turbulence. Simulation results are demonstrated for large pitch-roll maneuvers, and for maneuvers with failure of the right stabilator. There are substantial differences between the control law design and simulation models, which are used to demonstrate some robustness aspects of this control law. Actuator saturation is shown to be a considerable problem for this type of controller. However, the flexibility of the backstepping design provides opportunities for improvement. In particular, the Lyapunov function is modified so that the growth of integrated error and the rate of change of parameter growth are both reduced when the surface commands are growing at a rate that will likely saturate the actuators. In addition, the deadzone technique from robust linear adaptive control is applied to improve robustness to turbulence.

Introduction

In the early 1990's, adaptive backstepping was developed by Kanellakopoulos et al[1] as a way of designing stable adaptive control laws for a broad range of nonlinear systems. Adaptive backstepping is an approach that combines Lyapunov stability theory with the substantial advances made in nonlinear differential-geometric control theory[2] in the recent past. The basic concept behind backstepping is to use some states as virtual controls to control other states. However, this initial approach required overparameterization, and yielded high order controllers that were not very practical for most flight control problems. More recent work by Krstc et al[3-4] developed a tuning function approach to eliminate overparameterization. The tuning function approach adds computational complexity to the controller, but yields a controller of the same order as the number of unknown parameters. The primary benefit of this type of controller would seem to be that it allows a wide array of nonlinearities to be incorporated in the controller design, and has proven nominal stability and convergence of error. The types of nonlinearities included in the control law design could be either nonlinearities in the system model or nonlinearities chosen to meet the complex design criteria associated with flight control. In the past, such nonlinearities have not been very successful in flight control[5], but the powerful theoretical tools associated with backstepping may make such designs more feasible. Another potential advantage of backstepping is that it converges very quickly (when it does converge) because it does not have the lags associated with parameter identification for conventional adaptive control approaches. As a result, it may be effective in dealing with damage and failures. However, there are concerns about the robustness of backstepping designs. Even more problematic is that basic backstepping designs tend to generate very large effector commands. This is a serious problem for flight control, due to the importance of actuator saturations in aircraft. Luckily, the flexibility of backstepping design seems to provide opportunities to mitigate this problem. Freeman & Kokotovic[6] and Zhao & Kanellakopoulos[7], for example, provide some interesting approaches to reduce the magnitude of control commands generated by a backstepping control law.

In recent years, backstepping has been applied to a number of research problems including a 1 Degree-of-Freedom wing rock problem[8], electric motor control[9-

[1] Engineer, Senior Member AIAA
[2]Engineer, Member AIAA

[11],. engine control[12], robotics[13], neural network control[14], and ship control[15-16]. Another interesting approach towards nonlinear direct adaptive flight control is that of Kim & Calise[17], Leitner et al[18], and McFarland[19]. This approach uses neural networks, but provides theoretical proofs based on similar tools. Singh & Steinberg[20] developed a backstepping adaptive control law with increased robustness through the incorporation of integrated error in the Lyapunov function, and applied it to a simple nonlinear aircraft simulation. The aircraft simulation was a constant velocity model with no disturbances or actuator models. The main contribution of this paper is to demonstrate this adaptive backstepping approach on a much more complex simulation model, and modify the previous design to deal with turbulence and actuator saturations. Dealing with actuator saturations, in particular, provides a good venue to demonstrate the flexibility of backstepping design. The Lyapunov function from ref. 20 is modified to reduce integrated error growth and the rate of change of parameter estimates when the actuator command is approaching saturation. Also, in ref. 20,the only difference between the control law design model and the simulation model was that the lift and drag effects of the control surfaces were not taken into account in the design model. In this paper, there are many more differences from the simulation model, so the results in this paper examine the robustness of this control law to a wide range of errors in the model. Finally, the control law in this paper makes use of the deadzone technique from linear robust adaptive control[21] to improve robustness to turbulence.

Aircraft Simulation Model

The aircraft simulation being used is a high performance aircraft with 2 engines, 2 stabilators, 2 ailerons, 2 rudders, 2 leading edge flaps, and 2 trailing edge flaps. The simulation uses the standard equations of motion and kinematic relations[22]

$$\dot{u} = \frac{F_{X_A} + F_{X_T}}{m} - g\sin\Theta + rv - qw$$

$$\dot{v} = \frac{F_{Y_A} + F_{Y_T}}{m} + g\cos\Theta\sin\Phi + pw - ru$$

$$\dot{w} = \frac{F_{Z_A} + F_{Z_T}}{m} + g\cos\Theta\cos\Phi + qu - pv$$

$$\dot{p}\left(I_{XX}I_{ZZ} - I_{XZ}^2\right) = I_{ZZ}\left(l_A + l_T - qr\left(I_{ZZ} - I_{YY}\right) + qpI_{XZ}\right) + I_{XZ}\left(n_a + n_T + qp\left(I_{XX} - I_{YY}\right) - qrI_{XZ}\right)$$

$$\dot{q}\left(I_{YY}\right) = m_A + m_T + \left(r^2 - p^2\right)\left(I_{XZ}\right) + pr\left(I_{ZZ} - I_{XX}\right)$$

$$\dot{r}\left(I_{XX}I_{ZZ} - I_{XZ}^2\right) = I_{XX}\left(n_A + n_T + qp\left(I_{XX} - I_{YY}\right) - qrI_{XZ}\right) + I_{XZ}\left(l_a + l_T - qr\left(I_{ZZ} - I_{YY}\right) + qpI_{XZ}\right)$$

$$P = \dot{\Phi} - \dot{\Psi}\sin\Theta$$

$$Q = \dot{\Theta}\cos\Phi + \dot{\Psi}\cos\Theta\sin\Phi$$

$$R = \dot{\Psi}\cos\Theta\cos\Phi - \dot{\Theta}\sin\Phi$$

The components of the aerodynamic forces $(F_{x_a}, F_{y_a}, F_{z_a})$ and moments $(l_a, m_a, n_a)$are calculated from table look-ups. Gross thrust, T, is calculated from the following equation:

$$T = \left[1 + a_1\alpha + a_2\alpha^2\right]F_T(h, M, P_{LT})\left[kP_{LT} + c\right]$$

where a_1, a_2, c, and k are constants, F_T is calculated from a table look-up, and P_{LT} is lagged throttle position. The throttle model is a first order linear system with a variable time constant and variable rate limit based on the value of P_{LT}. The actuator models are 2nd order linear systems with rate and position limits. The turbulence model is the standard Dryden Gust model from MIL-STD-1797A[23].

Control Law Design Model

For purposes of design, the full simulation model would yield a control law that was far too complex to be practically implemented. Also, it was felt to be important to deliberately have some major differences between the design and simulation model in order to examine the robustness of the control law. As a result, the following model was used

$$\begin{pmatrix}\dot{p}\\ \dot{q}\\ \dot{r}\\ \dot{\alpha}\\ \dot{\beta}\\ \dot{\phi}\\ \dot{\theta}\end{pmatrix} = \begin{pmatrix} l_\beta\beta + l_q q + l_r r + (l_{\beta\alpha}\beta + l_{r\alpha} r)\Delta\alpha + l_p p - i_1 qr \\ \overline{m}_\alpha \Delta\alpha + \overline{m}_q q + i_2 pr - m_{\dot{\alpha}} p\beta + m_{\dot{\alpha}}(g_0 / V)(\cos\theta\cos\phi - \cos\theta_0) \\ n_\beta\beta + n_r r + n_p p + n_{p\alpha} p\Delta\alpha - i_3 pq + n_q q \\ q - p\beta + z_\alpha \Delta\alpha + (g_0 / V)(\cos\theta\cos\phi - \cos\theta_0) \\ y_\beta\beta + p(\sin\alpha_0 + \Delta\alpha) - r\cos\alpha_0 + (g_0 / V)\cos\theta\sin\phi \\ p + q\tan\theta\sin\phi + r\tan\theta\cos\phi \\ q\cos\phi - r\sin\theta \end{pmatrix}$$

$$+ \begin{pmatrix} l_{\delta a} + l_{\alpha\delta a}\Delta\alpha & l_{\delta r} & 0 \\ 0 & 0 & \overline{m}_{\delta e} \\ n_{\delta a} + n_{\alpha\delta a}\Delta\alpha & n_{\delta r} & 0 \\ 0 & 0 & 0 \\ 0 & 0 & 0 \\ 0 & 0 & 0 \\ 0 & 0 & 0 \end{pmatrix} \begin{pmatrix}\delta_a \\ \delta_r \\ \delta_e\end{pmatrix}$$

Some of the key simplifications made in this model are constant velocity (a separate auto-throttle will attempt to maintain this), no lift and drag effects of the control surfaces, and none of the higher frequency dynamics (e.g., actuators). Also, the stabilators and rudders will only be used collectively, and the effects of flaps, which are scheduled with Mach and angle-of-attack, are ignored.

Backstepping Control Law Design

This design roughly follows that of ref. 20 and for more detail the reader should consult that reference. However, there are several differences from that controller. First of all, the Lyapunov function is modified so that integrated error growth and the rate of change of unknown parameters are reduced when the actuators seem likely to saturate. Secondly, several scalar constants are turned into constant matrices. Third, all controller parameters are frozen if the actuators saturate, and the actuator error continues to increase. Finally, a deadzone is used to improve the robustness of the system to disturbances. The latter 2 changes have not yet been justified theoretically for the backstepping design, but have been for linear adaptive control designs[21].

Following [20], the aircraft equations of motion can be put in the form

$$\dot{y} = \Phi_0(x_1) + \Phi(x_1)w_1 + B_i(x_1)\omega$$
$$\dot{\omega} = \psi_0(x) + \psi_1(\xi)w_2 + D(\xi, w_u)u$$
$$\dot{\eta} = q_0(x) + q_1(\xi)w + q_2(\xi, w_u)u$$

In this form, y is a vector of the outputs that will be controlled, ω is the virtual control vector used to control y, η is the vector of uncontrolled states, w_1, w_2, and w_u are the vectors of unknown parameters, x_1 is a subset of the state vector, and u is the vector of control effector commands where

$$y = (\phi, \alpha, \beta)^T$$
$$\omega = (p, q, r)^T$$
$$\eta = \theta$$
$$x_1 = (\alpha, \beta, \phi, \theta)$$
$$w_1 = (z_\alpha, y_\beta)^T$$
$$w_2 = (l_\beta, l_p, l_q, l_r, l_{\beta\alpha}, l_{r\alpha}, \overline{m}_\alpha, \overline{m}_q, m_{\dot{\alpha}}, n_\beta, n_r, n_p, n_{p\alpha}, n_q)^T$$
$$w_u = (l_{\delta a}, l_{\alpha\delta a}, l_{\delta r}, \overline{m}_{\delta e}, n_{\delta a}, n_{\alpha\delta a}, n_{\delta r})^T$$

We will next define the error, e, and a function s that combines error and integrated error

$$e = y - y_c$$
$$s = e + K_0 x_s$$
$$\dot{x}_s = f_c e$$

where K_0 is a positive definite symetric matrix and y_c is the output of a command generator that is a linear, stable 3rd order system. The function f_c is a scalar bounded, twice differentiable, positive function with bounded derivatives that normally equals 1, but will be decreased to reduce the growth of integrated error when the actuators are approaching saturation. Choice of f_c will be discussed in greater detail below. Taking the derivative of s yields

$$\dot{s} = \Phi(x_1)w_1 + B(x_1)(\omega_d + \tilde{\omega}) + v$$
$$\omega = \omega_d + \tilde{\omega}$$
$$v = \Phi_0 - \dot{y}_c + K_0 f_c e$$

In this equation, ω_d represents the desired value of the virtual controls. However, since these are states and not directly controllable effectors, there will be an error $\tilde{\omega}$.

We will next choose ω_d through the use of the following Lyapunov function

$$U_1 = (s^T f_c s + \tilde{w}_1^T L_1 \tilde{w}_1)/2$$
$$\tilde{w}_i = w_i - \hat{w}_i$$

where L_1 is a positive definite diagonal matrix and $\hat{w}_i$ is the estimate of w_i.
Taking the derivative of U_1 yields

$$\dot{U}_1 = s^T f_c\left[\Phi(x_1)w_1 + B(x_1)(\tilde{\omega} + \omega_d) + v(x_1, \dot{y}_c, f_c)\right] + \tilde{w}_1^T L_1 \tilde{w}_1 + \dot{f}_c s^T s$$

ω_d can then be chosen as

$$\omega_d = B^{-1}(x_1)[-K_{11}s - \Phi^T(x_1)\hat{w}_1 - v(x_1, \dot{y}_c, f_c)]$$

where K_{11} is a positive definite diagonal matrix.
As a result of that choice of ω_d

$$\dot{U}_1 = -(K_{11}f_c - \dot{f}_c)s^T s + \tilde{w}_1^T\left[f_c\Phi^T s + L_1\dot{\tilde{w}}_1\right] + f_c\tilde{\omega}^T B^T(x_1)s$$

If we put $\dot{\omega}_d$ in the form

$$\dot{\omega}_d = \psi_{od} - \psi_{1d}w_1 + \psi_{2d}w_2$$

then,

$$\dot{\tilde{\omega}} = \psi_{0a} + \psi_{1a}\hat{w}_1 + \psi_{2a}\tilde{w}_2 + D(x, w_u)u$$
$$\psi_{0a} = \psi_0 - \psi_{0d} + \psi_{1d}\hat{w}_1 + \psi_{2a}\hat{w}_2$$
$$\psi_{1a} = \psi_{1d}$$
$$\psi_{2a} = \psi_1 - \psi_{2d}$$

We will next chose a 2nd Lyapunov function such that

$$U_2 = U_1 + (\tilde{\omega}^T f_c\tilde{\omega} + \tilde{w}_2^T L_2\tilde{w}_2 + \tilde{w}_u^T L_3\tilde{w}_u + x_\omega^T K_{33}x_\omega)/2$$

where L_1, L_2, and K_{33} are all positive definite diagonal matrices and $\dot{x}_w$ is given by

$$\dot{x}_w = f_c\tilde{\omega}$$

Taking the derivative of U_2 gives

$$\dot{U}_2 = -(K_{11}f_c - \dot{f}_c)s^T s + \tilde{w}_1^T\left[f_c\Phi^T s + L_1\dot{\tilde{w}}_1 + f_c\psi_{1a}^T\tilde{\omega}\right] + \tilde{w}_2\left[L_2\dot{\tilde{w}}_2 + f_c\psi_{2a}^T\tilde{\omega}\right] + \tilde{w}_u^T L_3\dot{\tilde{w}}_u$$
$$+\tilde{\omega}^T f_c\left[B^T s + \psi_{0a} + Du + K_{33}x_\omega\right] + \dot{f}_c\tilde{\omega}^T\tilde{\omega}$$

We will next chose the following control law

$$u = \hat{D}^{-1}(-B^T s - (\psi_0 - \psi_{0d} + \psi_{1d}\hat{w}_1 + (\psi_1 - \psi_{2d})\hat{w}_2) - K_{22}\tilde{\omega} - K_{33}x_\omega)$$
$$\dot{\hat{w}}_1 = f_c L_1^{-1}(\Phi^T s + (\psi_{1d}^T\tilde{\omega})$$
$$\dot{\hat{w}}_2 = f_c L_2^{-1}\psi_{2a}^T\tilde{\omega}$$
$$\dot{\hat{w}}_u = f_c L_3^{-1}\Psi_u^T\tilde{\omega}$$

where Ψ_u is chosen so

$$[D(x, w_u) - D(x, \hat{w}_u)] = \Psi_u(x, u)\tilde{w}_u$$

As a result, since K_{11} and K_{22} are postive definite diagonal matrices and f_c is always positive, then, if f_c is chosen correctly

$$\dot{U}_2 = -(K_{11}f_c - \dot{f}_c)s^T s - (K_{22}f - \dot{f}_{cc})\tilde{\omega}^T\tilde{\omega} \le 0$$

Following the approach of ref. 20, it can be shown that the for the nominal system, s, $\tilde{\omega}$, and e all tend to zero as $t \to \infty$.

f_c is made up of 2 components. The first is a fuzzy logic component and the second is a 3rd order linear stable system, chosen such that $\dot{f}_c$ meets the above requirements for the range of possible inputs from the fuzzy logic system f_{in}. Fuzzy logic was used because it is an easy to design way of building a function to transition from 1 to the minimum value of f_{in}. The fuzzy logic rules are as follows:

1) If actuator position is normal and actuator rate is normal, then f_{in} is normal (i.e., 1)

2) If (actuator position is large or actuator rate is fast) and s is increasing rapidly, then f_{in} is medium

3) If (actuactor position is very large or actuator rate is very fast) and s is increasing, then f_{in} is medium

4) If (actuactor position is very large or actuator rate is very fast) and s is increasing rapidly, then f_{in} is small

5) If (actuator position is near saturation or actuator rate is near saturation) and (s is increasing or increasing rapidly), then f_{in} is small

In addition, if the actuator saturates and filtered actuator error is increasing above a threshold value, then f_c is immediately set to zero. This violates the above stability proof, but is necessary to prevent departures in some situations.

Simulation Results

All simulation results were generated by Matlab/Simulink v. 4.2.1 using the RK45 integration routine and the full nonlinear simulation model with actuator and engine models.

Fig. 1 demonstrates the performance of the control law making a combined 60 degree roll and 8 degree angle-of-attack change while attempting to maintain zero sideslip at Mach .5 and 45,000 ft. altitude with no turbulence. The solid lines are the commanded values and the dotted lines are the actual values. This is a particularly difficult flight condition for the controller because the low dynamic pressure can lead to large control magnitudes that could saturate the actuators. As you can see, the roll response is very good. The alpha response is not quite as good, but this is partly due to the fact that the auto-throttle was not perfect and the velocity was fluctuating during the maneuver. There is some slight saturation of the rudder actuator. However, this is much less than would occur with the basic control law of ref. 20 without the actuator saturation mitigation approach of this paper. Fig. 2 shows the desired and actual values of the virtual control inputs for this case. Fig. 3 shows what happens for this same scenario, with f_c=1 at all times. In this case, the actuators rapidly saturate, and the aircraft departs. Of course, with this initial control law, smaller gains could have been used. However, the use of smaller gains led to very poor tracking performance throughout the envelope.

Figure 4 shows the same maneuver at the same flight condition with a failure of the right stabilator at 1.5 seconds. There is only fairly slight degradation of the roll and sideslip response and modest degradation of the alpha response. The reason for the good response can be seen in Fig. 5, which shows the change in estimated stab effectiveness. Due to the lack of filters, the parameter converges to a new reduced value very rapidly after the failure at 1.5 sec.

Tables 1 through 3 provide some error statistics for a 180 degree roll with an 8 degree angle-of-attack change followed by a return to the initial roll and angle-of-attack angles while attempting to maintain zero sideslip in moderate turbulence, as defined in MIL-STD-1797 [22]. The controller performs acceptably at all flight conditions. As mentioned earlier, the low dynamic pressure condition had the most difficulties with departures due to actuator saturation, but the high dynamic pressure condition has the worst tracking errors.

Despite the improvements made in mitigating the impact of actuator saturationsthrough the f_c function, the control law still cannot be used for very fast maneuvers. Fig. 6 shows an attempt to command a much faster roll. In this case, the actuators saturate despite the use of f_c and cause the aircraft to depart

Conclusions

This paper demonstrates an adaptive backstepping flight control law on a complex high performance aircraft simulation. The control law is demonstrated to have very fast convergence properties and to provide good performance in many situations, including the loss of a stabilator. It also demonstrated good robustness properties to a wide range of modelling errors. However, more work needs to be done to reduce the magnitudes of actuator commands, while still maintaining good performance. Achieving good performance generally required limiting the commands to the controller to prevent departure. Some of the potential ways of dealing with this could include better control allocation, improvements in the use of the f_c function, and changes in the Lyapunov function to reduce the effective gain of the system or to modify the gain based on dynamic pressure. Luckily, backstepping design provides considerable flexibility to alter the Lyapunov function in such ways. However, it is usually not clear what effect many changes will have on the system and better theoretical tools and further simulation will be required.

References

[1]Kanellakopoulos, I., Kokotovic, P.V., and Morse, A.S., "Systematic Design of Adaptive Controllers for Feedback Linearizable Systems," *IEEE Transactions on Automatic Control*, Vol. 36, 1991, pp. 1241-1253.

[2]Isadori, A., *Nonlinear Control Systems*, Springer-Verlag, Berlin, second ed., 1989.

[3] Krstic, M., Kanellakopoulus, I., and Kokotovic, P.V., "Adaptive Nonlinear Control without Overparameterization," *Systems and Control Letters*, Vol. 19, 1992, pp. 177-185.

[4]Krstic, M., Kanellakopoulus, I., and Kokotovic, P.V, *Nonlinear and Adaptive Control Design*, John Wiley and Sons, New York, 1995.

[5] Graham, D., and McRuer, D., "Retrospective Essay on Nonlinearities in Aircraft Flight Control," Journal of Guidance, Control, and Dynamics, Vol. 14, No. 6, 1991, pp. 1089-1099

[6]Freeman, R.A., Kokotovic, P.V., *Robust Nonlinear Control Design: State Space and Lyapunov Techniques*, Birkhauser, Boston, 1996.

[7]Zhao, J., Kanellakopoulos, I., "Flexible Backstepping Design for Tracking and Disturbance Attenuation," *International Journal of Control*, to appear.
[8]Monahemi, M.M. and Krstic, M., "Control of Wing Rock Motion Using Adaptive Feedback Linearization," *Journal of Guidance, Control, and Dynamics*, Vol. 13, No. 6, 1990, pp. 905-912.
[9]Dawson, D.M., Carroll, J.J., and Schneider, M., "Integrator Backstepping Control of a Brush DC Motor Turning a Robotic Load," *IEEE Transactions on Control Systems Technology*, Vol. 2, No. 3, 1994, pp. 233-244.
[10]Milman, R., "Adaptive Backstepping Control of the Variable Reluctance Motor," M.S. Thesis, University of Toronto, 1997.
[11]Caroll, J.J., Dawson, D.M., and Qu, Z., "Adaptive Tracking Control of a Switched Reluctance Motor Turning an Inertial Load," Proceedings of the American Control Conference, 1993, pp. 670-674.
12
[13]Lim, S.Y., Dawson, D.M., Anderson, K., "Re-Examining the Nicosia-Tomei Robot Observer-Controller from a Backstepping Perspective, IEEE Transaction on Control Systems Technology, Vol. 4, No. 3, 1996, pp. 304-310.
[14]Kwan, C.M. and Lewis, F.L., "Robust Backstepping Control of Nonlinear Systems Using Neural Networks," *Proceedings of the European Control Conference*, 1995, pp. 2772-2777.
[15]Fossen, T.I., Grovlen, A. "Nonlinear Output Feedback Control of Dynamically Positioned Ships Using Vectorial Observor Backstepping," IEEE Transactions on Control Systems Technology, Vol. 6, No. 1, 1998, pp. 121-128.
[16]Knut, E.H., Fossen, T.I., "Backstepping Designs for Nonlinear Way-Point Tracking of Ships," presented at Conference on Manoeuvering and Control of Marine Craft, 1997.
[17]Kim, B.S., and Calise, A.J., "Nonlinear Flight Control Using Neural Networks,"
AIAA Journal of Guidance, Control, and Dynamics, Vol. 20, No. 1, 1997.
[18]Leitner, J., Calise, A., and Prasad, J. V. R., "Analysis of Adaptive Neural Networks for Helicopter Flight Controls," *AIAA Journal of Guidance, Control, and Dynamics*, Vol. 20, No. 5, 1997.
[19] McFarland, M., *Adaptive Nonlinear Control of Missiles Using Neural Networks*,
Ph.D. thesis, Georgia Institute of technology, Atlanta, GA, July 1997.
[20]Singh, S.N. and Steinberg, M., "Adaptive Control of Feedback Linearizable Nonlinear Systems with Application to Flight Control, *Journal of Guidance, Control, and Dynamics*, Vol. 13, No. 6, 1990, pp. 871-877.
[21]Ioannou, P. and Sun, J., *Robust Adaptive Control*, Prentice-Hall, New Jersey, 1996.
22
[23]MIL-STD-1797A, Military Standard, Flying Qualities of Piloted Aircraft, 30 January, 1990.

Table 1 - Mach .7, 30K ft altitude

	Average Absolute Error	Maximum Absolute Error
Phi (deg.)	.74	1.9
Alpha (deg.)	.67	1.2
Beta (deg.)	.43	1.4

Table 2 - Mach .9, 5K ft altitude

	Average Absolute Error	Maximum Absolute Error
Phi (deg.)	1.8	4.7
Alpha (deg.)	0.93	2.1
Beta (deg.)	0.87	2.8

Table 3 - Mach .5, 45K altitude

	Average Absolute Error	Maximum Absolute Error
Phi (deg.)	0.71	2.6
Alpha (deg.)	0.64	2.2
Beta (deg.)	0.49	2.4

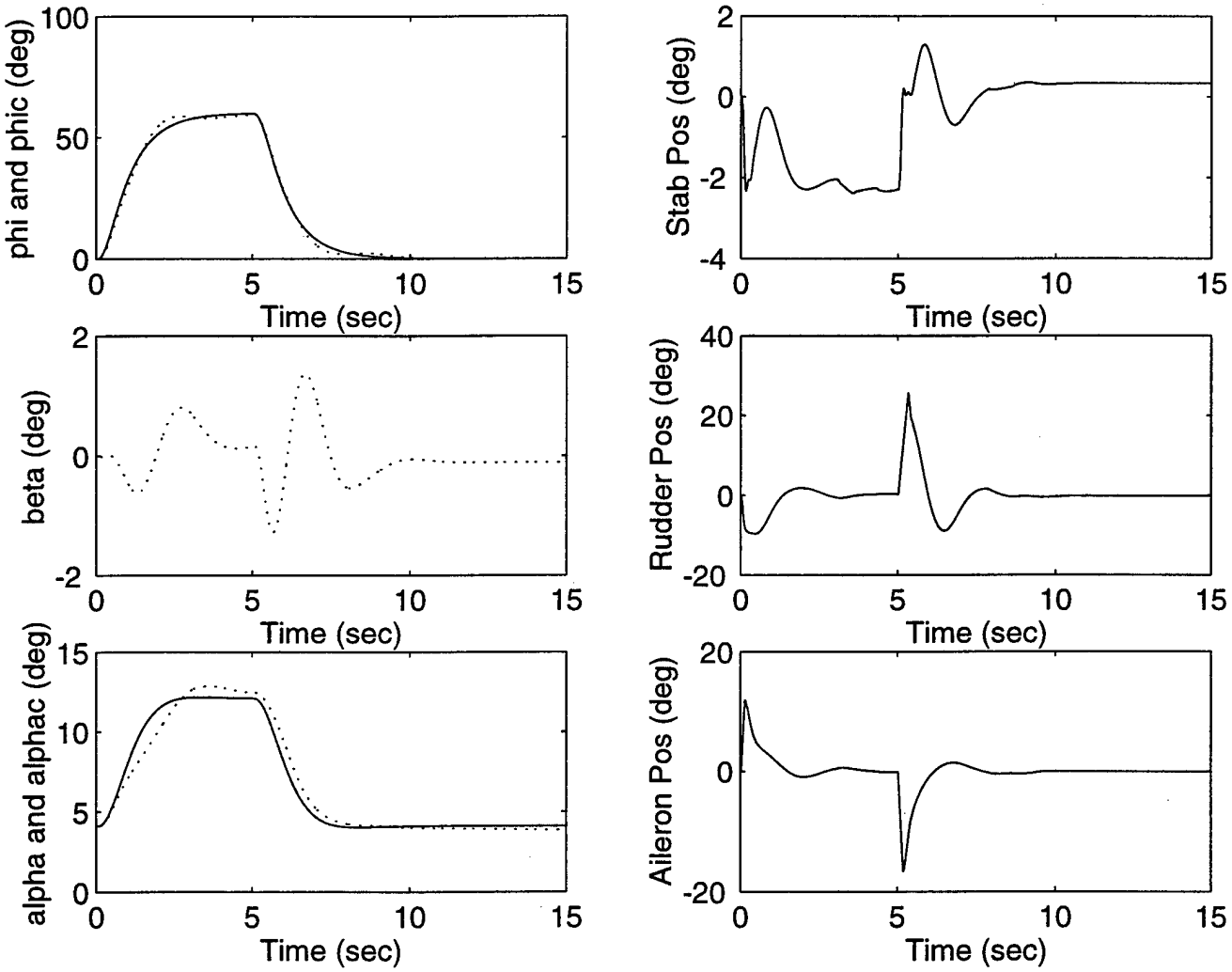

Figure 1 - No Failure Case with Actuator Saturation Mitigation Activated

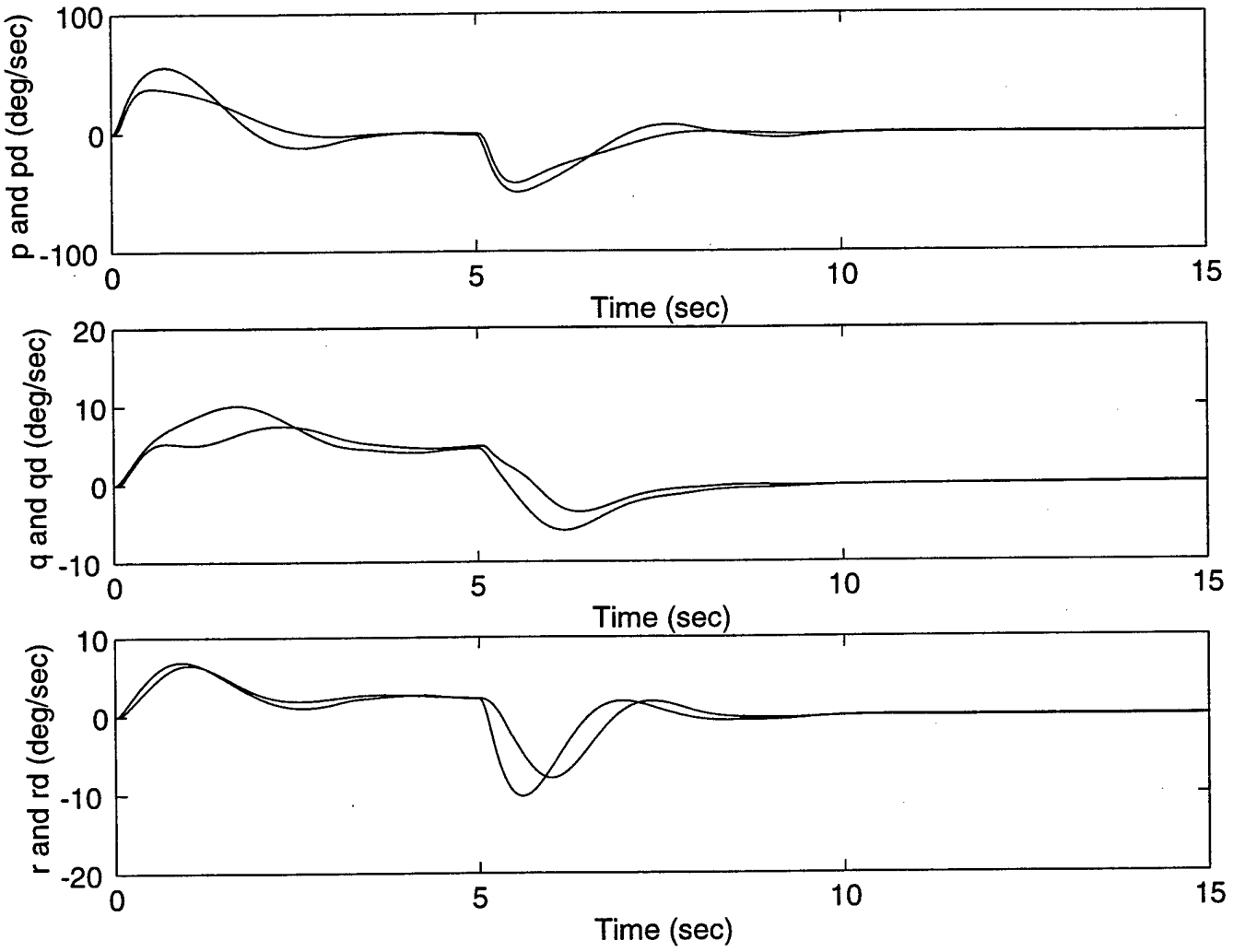

Figure 2 - Desired and Actual Values of Virtual Controls for No Failure C

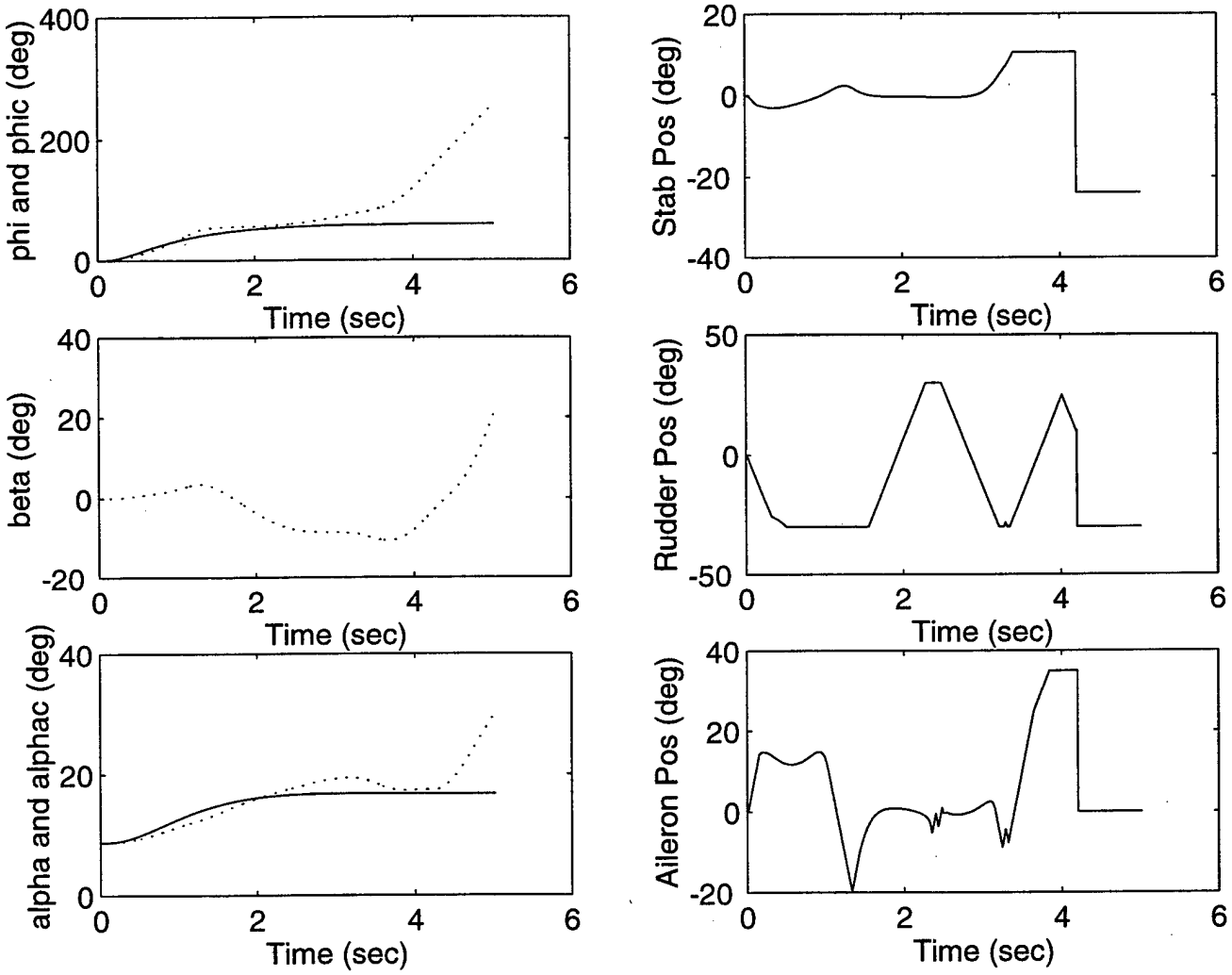

Figure 3 - No Failure Case without Actuator Saturation Mitigation

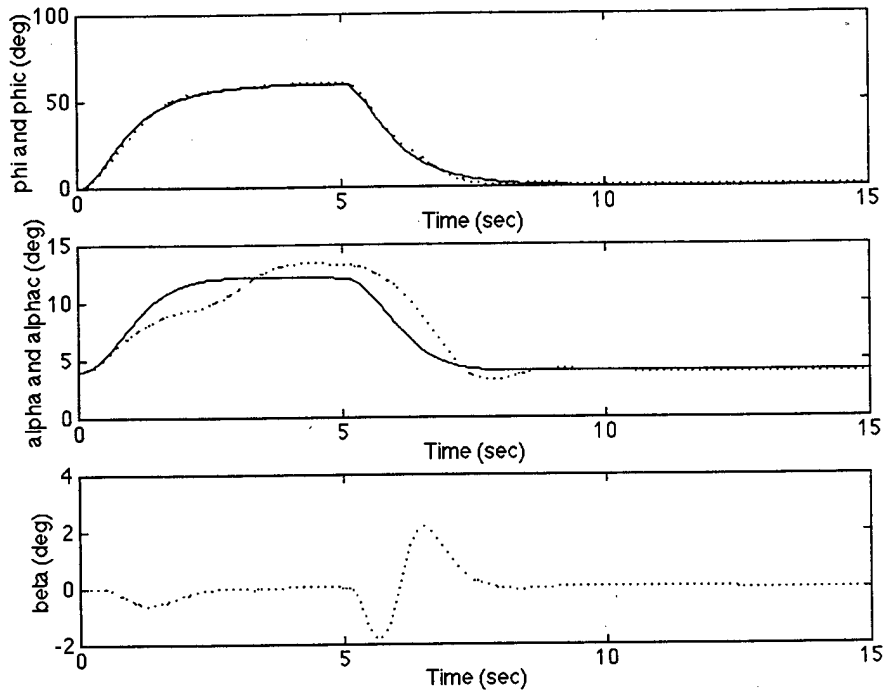

Figure 4 - Stabilator Failure Case

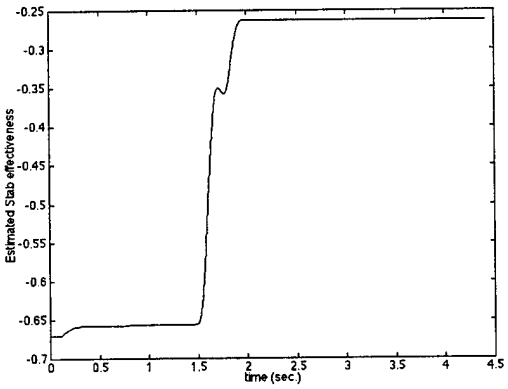

Figure 5 - Stabilator Effectiveness Estimate at failure

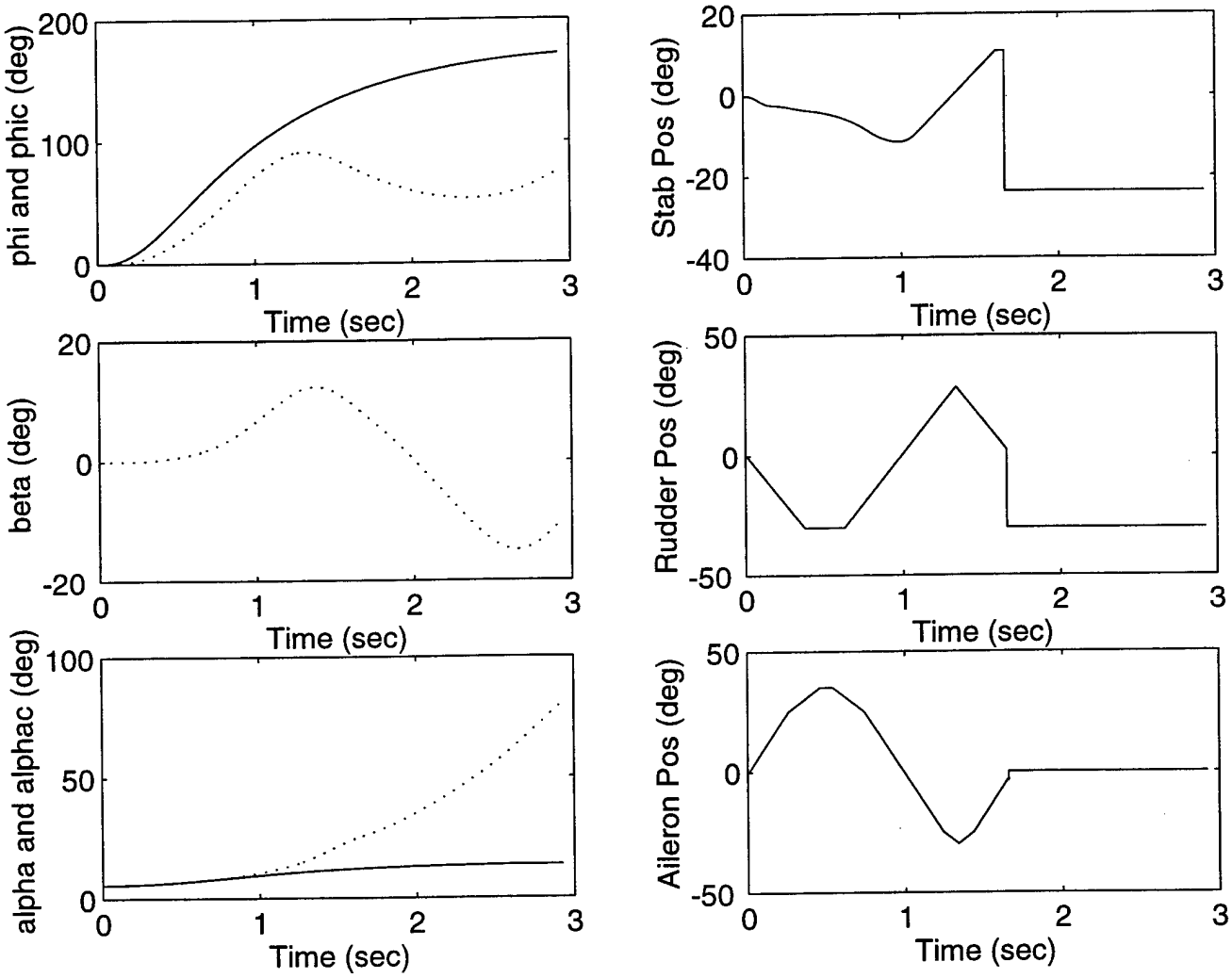

Figure 6 - Very Fast Roll Command